Published October 14, 2014

Original Research

A Modified Philip–Dunne Infiltrometer for Measuring the Field-Saturated Hydraulic Conductivity of Surface Soil

F. Ahmed, R. Nestingen, J.L. Nieber,* J.S. Gulliver, and R.M. Hozalski

There is a current and expanding need to measure surface infiltration rate parameters for stormwater infiltration practices used to mitigate the detrimental effects of land development activities on watershed hydrology. We have developed a falling-head soil surface infiltrometer, termed the modified Philip–Dunne (MPD) infiltrometer, that is inexpensive to construct, easy to use, and requires a minimal water volume per test. Because of these characteristics, many MPD devices can be deployed simultaneously to obtain infiltration rate data at multiple locations within a given infiltration practice. Green–Ampt theory was used to derive the expressions needed for analyzing the falling-head data to solve for the field-saturated hydraulic conductivity (K_{fs}) and Green–Ampt wetting-front suction (ψ). The accuracy of the analysis was determined using numerical experiments in which falling-head data were generated from a computational solution of the axisymmetric form of the three-dimensional Richards' equation for homogeneous and isotropic porous media with specified input parameters. The falling-head data were then analyzed using a quasi-analytical procedure, and the resulting values of K_{fs} and ψ were compared with the input values. The accuracy of K_{fs} and ψ derived from data acquired using the MPD device was then assessed using physical experiments involving three large barrels packed with different types of sand. The K_{fs} values obtained for the media in the barrels using an MPD infiltrometer were, on average, 82% of the values obtained from whole barrel falling-head tests. The resulting uncertainty in K_{fs} values from the MPD infiltrometer is considered to be small compared with the orders of magnitude of variability commonly observed for K_{fs} values in the field.

Abbreviations: MPD, modified Philip–Dunne.

A new falling-head infiltrometer method is presented for estimating field-saturated hydraulic conductivity and Green–Ampt wetting front suction for soil surfaces. The method was verified using referenced laboratory columns, and falling-head data were generated synthetically using Richards' equation solutions for axisymmetric flow.

F. Ahmed, J.S. Gulliver, and R.M. Hozalski, Dep. of Civil, Environmental and Geo-engineering, Univ. of Minnesota, Minneapolis, MN 55414; R. Nestingen, Short Eliott Hendrickson, Inc., 3535 Vadnais Center Drive, St. Paul, MN 55110; and J.L. Nieber, Dep. of Bioproduct and Biosystem Engineering, Univ. of Minnesota, St. Paul, MN 55108. *Corresponding author (nieber@umn.edu).

Vadose Zone J.
doi:10.2136/vzj2014.01.0012
Received 30 Jan. 2014.
Supplemental material online.

Infiltration basins, rain gardens, swales, and other infiltration practices are stormwater control measures that reduce runoff volume through means of infiltration and evapotranspiration, of which infiltration is the most significant. If infiltration is not occurring at a sufficient rate, the capacity to reduce runoff volume is decreased, potentially leading to increased pollutant discharge, increased degradation of stream channels, and increased potential for flooding of downstream areas. The surfaces of infiltration practices are prone to compaction (Olson et al., 2013) due to foot and equipment traffic as well as clogging from the fine particles typically transported in stormwater runoff. To evaluate the impacts of compaction and particle accumulation, it is important to measure the field-saturated hydraulic conductivity of the media at the surface because it is the main determinant of the infiltration capacity of a particular soil.

Field-saturated hydraulic conductivity (K_{fs}) is the most important soil property that controls water infiltration and consequently surface runoff. Methods to determine this soil property can be placed into two main categories: methods based on steady-state infiltration and methods based on unsteady infiltration. Within these categories there are subcategories that relate to the type of geometric and pressure boundary conditions imposed. The

common types of geometries include boreholes, surface disks, and surface rings. Pressures applied at the soil boundary can be positive, zero, or negative. Of interest in this study is a type of measurement that will yield the hydraulic properties of the soil surface. For this, several methods have been developed, with water application geometries that include disk infiltrometers, single-ring infiltrometers, and double-ring infiltrometers (ASTM, 2003) applied for steady-state flow or for unsteady flow (Parr and Bertrand, 1960; Reynolds and Elrick, 1990; Bagarello et al., 2004; Lassabatere et al., 2006; Reynolds, 2008; Nimmo et al., 2009).

It has been found that, both for field soils and for infiltration practices, the K_{fs} of a medium can vary spatially up to two orders of magnitude (Asleson et al., 2009; Olson et al., 2010, 2013). To capture the spatial variability of K_{fs} and to determine a representative infiltration capacity, a large number of measurements are required to represent field conditions. This situation calls for measurement methods that are quick, require the least amount of water, and are relatively easy to set up. To meet time constraints on projects, it is also desirable if the measurements can be made simultaneously at multiple sites by a single practitioner. This almost certainly requires that the methods involve measurement of short-term unsteady infiltration. To meet this data collection requirement for our own needs of data collection, we developed and tested a modified version of the Philip–Dunne borehole permeameter (referred to as the modified Philip–Dunne infiltrometer or MPD infiltrometer). The device is simple, inexpensive to construct, and has low water volume requirements per test; hence, 20 or more devices can be deployed to measure the soil hydraulic parameters at as many different locations simultaneously. The MPD infiltrometer requires ~0.003 m^3 of water per test, while the most commonly used device, the double-ring infiltrometer, requires ~0.028 m^3 of water (Ahmed et al., 2011).

The falling-head Philip–Dunne permeameter is inserted into a borehole to a given depth and is used to obtain the K_{fs} and Green–Ampt wetting-front suction (ψ) of the soil at that depth. It cannot be used to measure K_{fs} and ψ at the soil surface of an infiltration practice. In contrast, the MPD infiltrometer is not inserted into a borehole but is driven into the soil surface to a specified depth without removing any soil. Because this modification changes the boundary conditions applied to the infiltrating flow compared with the conditions associated with the Philip–Dunne borehole permeameter, it is not possible to use the approximate borehole infiltration analysis of Philip (1993) to derive the hydraulic properties of the soil. Philip's analysis, however, can be modified to arrive at a similar approach for analyzing the head vs. time data collected from the MPD infiltrometer.

Three fairly recent studies that describe alternative approaches to the one we present here are those by Bagarello et al. (2004), Lassabatere et al. (2006), and Nimmo et al. (2009). The approach of Bagarello et al. (2004) applies the one-dimensional Green–Ampt formulation of Philip (1992) to analyze infiltration into an inserted ring infiltrometer. The approach of Lassabatere et al. (2006) fits a two-term infiltration formula to cumulative infiltration measurements to derive soil hydraulic property scale parameters and also a pedotransfer function approach with particle size distribution to derive shape parameters to describe the porous medium water retention and unsaturated hydraulic conductivity functions. The approach of Nimmo et al. (2009) uses a single-ring infiltrometer inserted into the soil and measures the time required for ponded water to infiltrate into the soil. The data analysis with this approach involves a single simple formula for field-saturated hydraulic conductivity. The formula contains a capillarity parameter, but this is assumed to be known or can be estimated for a particular soil type. Of these three methods the one of Nimmo et al. (2009) appears to be the closest, in terms of simplicity and ease of use, to the technique presented here.

The accuracy of the MPD infiltrometer, which was used to measure K_{fs} and ψ, was verified using numerical experiments and physical laboratory experiments.

Theory

In our application, the MPD infiltrometer was a 0.1-m-diameter cylinder that is driven 0.05 m into the soil, although these dimensions are free to be selected by the user. The initial moisture content of the soil near the surface is measured, and this initial moisture content is assumed to represent the initial moisture content of the underlying soil profile. The infiltrometer is then filled with water to a specified level, and the water level in the cylinder is monitored with time. The test continues until sufficient measurements of water surface elevation vs. time have been taken to estimate K_{fs}, usually until the water has completely emptied out of the infiltrometer cylinder.

The analysis of Philip (1993) was based on the assumptions of the Green–Ampt model. The soil was assumed to be an isotropic and homogeneous porous medium and the wetting front to be sharp and to represent the three-dimensional flow that was assumed as an ideal spherical geometry for the wetting front by considering symmetrical pressure-capillarity flow and superimposing a symmetrical gravity flow. He found that having a spherical source geometry had little influence on estimates of K_{fs} and ψ, which was of primary concern in our analysis.

A similar approach was taken for the analysis of the MPD infiltrometer. However, due to the application of the device at the surface rather than in a borehole, the no-flow boundary at the soil surface outside of the cylinder was taken into account by representing the wetted soil as a capped sphere, as illustrated in Fig. 1. In addition to modifying the geometry of flow, the pressure loss along the soil encased within the inserted portion of the device needed to be added into the analysis.

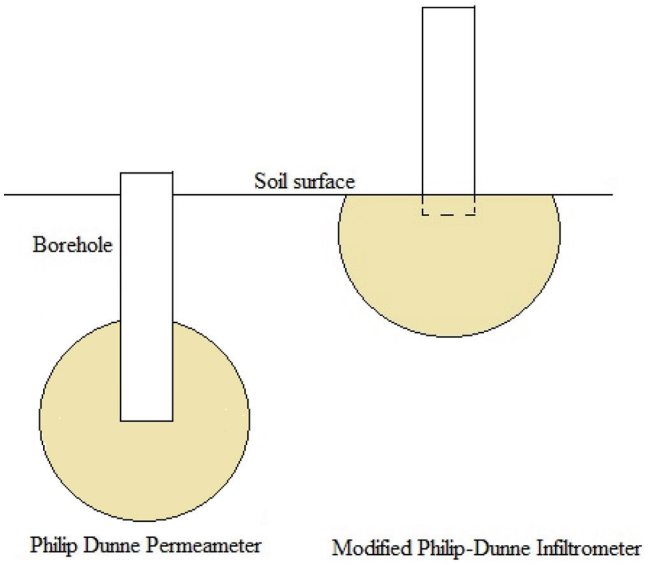

Fig. 1. Comparison of assumed wetted cross-sections for the Philip–Dunne permeameter and the modified Philip–Dunne infiltrometer.

Equation Modifications

The derivation of the governing equations for the MPD infiltrometer was based on the work of Nestingen (2007). The notation used in the derivation is illustrated in Fig. 2. Using similar assumptions as Philip (1993), the equation for cumulative infiltration, $i(t)$, is expressed by an equation using the geometry of the wetting front, which is a capped sphere with a radius of $R(t)$ and centroid at a vertical distance of L_{max} from the soil surface at the center of the cylinder $R(t) + L_{max}$. The soil within the capped sphere has initial and field saturated moisture contents of θ_i and θ_s, respectively. The total volume of the wetted soil matrix is calculated by subtracting the volume of the equivalent spherical source $(4/3)\pi r_o^3$, where $r_o = r_1/2$ is the radius of an equivalent spherical source, from the volume of the capped sphere defined by the advancing wetting front. The volume of the capped sphere bounded by the wetting front is $(\pi/3)[R(t) + L_{max}]^2\{3R^2(t) - [R(t) + L_{max}]\}$, where $R(t)$ is the sphere radius to the wetting front and L_{max} is the distance that the infiltrometer penetrates the soil. Thus the equation for temporal cumulative infiltration is

$$i(t)=\frac{\pi}{3}(\theta_s-\theta_i)\left[2R^3(t)+3R^2(t)L_{max}-L_{max}^3-4r_o^3\right] \quad [1]$$

A mass balance of the water remaining in the infiltrometer and the water that has infiltrated into the soil at a given time is used to compute $R(t)$ as a function of $H(t)$ for use in the analysis, replacing $i(t)$ with $[H_i - H(t)]\pi r_1^2$, where H_i is the initial height and $H(t)$ is the depth of water in the cylinder above the soil surface with time. With this we can now rewrite Eq. [1] to establish a relation between $H(t)$ and $R(t)$:

$$\left[H_i-H(t)\right]\pi r_1^2 = \frac{\pi}{3}(\theta_s-\theta_i)\left[2R^3(t)+3R^2(t)L_{max}-L_{max}^3-4r_o^3\right] \quad [2]$$

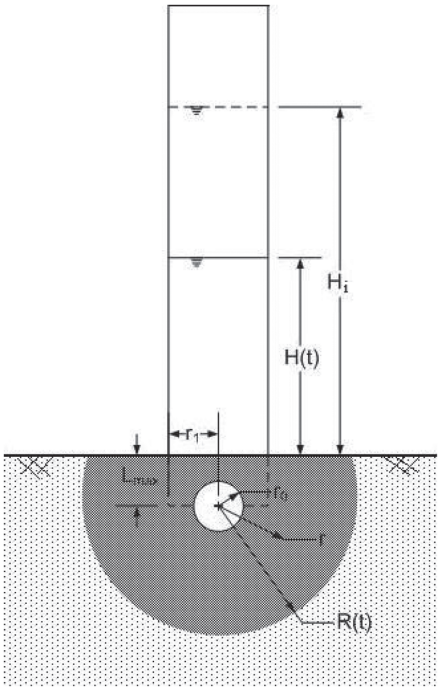

Fig. 2. Important parameters of the modified Philip–Dunne infiltrometer, including the initial height of water (H_i), the height of water at time t [$H(t)$], the depth of insertion into the soil (L_{max}), the equivalent source radius (r_0), the radius of the cylinder (r_1), any radius within the wetted front (r), and the radius to the sharp wetted front at time t [$R(t)$].

Equations [1] and [2] are applicable only after $R(t)$ is greater than the value $\sqrt{(r_1^2 + L_{max}^2)}$. The head vs. time data before the wetted zone reaches this minimum radius are neglected from the analysis because this is a point where the geometric shape for the problem becomes constant for the remainder of the experiment. Up to that point, the geometry has changed from one-dimensional flow along the encased cylinder of soil, and then to a sphere that grew until the top part of the sphere intersected with the soil surface and the geometry became that of a capped sphere. It would be possible to account for these intermediate changing geometries within the analysis if the equation set were expanded, but for the present the analysis we have limited ourselves to the formulation using Eq. [2].

Following the analysis procedure of Philip (1993), which involves differentiating Eq. [2] with respect to time, then separating the velocity into two components, a pressure-capillary-driven flow and a gravity-driven flow, the pressure-capillary flow velocity component, $v_c(r)$ at r between r_o and $R(t)$ becomes

$$v_c(r)=v_{co}\left(\frac{2r_o^2}{r^2+rL_{max}}\right) =\left\{(\theta_s-\theta_i)\left[R^2(t)+R(t)L_{max}\right]\frac{dR}{dt}-2r_o^2K_{fs}\right\} \times\frac{1}{r^2+rL_{max}} \quad [3]$$

where the gravity-driven flow term is given by $2r_o^2K_{fs}$. Applying Darcy's law, the pressure-capillarity potential drop, ΔP, from the spherical source to the wetted front is given by $\Delta P = \beta \int_{r_o}^{R(t)} [v_c(r)/K_{fs}]dr$, which can be evaluated to give

$$\Delta P = \beta \int_{r_o}^{R(t)} \frac{v_c(r)}{K_{fs}} dr = \beta \left[(\theta_s - \theta_i) \frac{R^2(t) + R(t)L_{max}}{K_{fs}} \frac{dR}{dt} B - G \right] \quad [4]$$

where β is a coefficient that takes into account the hydraulic inefficiency of the actual flow path of infiltrated water into the soil, $B = (1/L_{max})(\ln\{R(t)(r_o + L_{max})/r_o[R(t) + L_{max}]\})$, and $G = 2r_o^2B$ is the term arising from the gravity-driven component of the flow. Through an exploratory analysis, Philip (1993) estimated the β coefficient to be $\pi^2/8$, which is used here.

The use of G for the gravity term follows from the analysis of Reynolds (2011), who showed that, at $t = 0$ for the Philip–Dunne borehole permeameter, the gravity term is equal to zero, while at large time (if the volume of water in the permeameter tube is unlimited), the gravity term converges on r_o. For the MPD infiltrometer, the gravity term is zero at $t = 0$. while at large time the term converges on $2r_o^2/L_{max}\ln(1 + L_{max}/r_o)$.

To calculate the pressure, $P_o(t)$, at the surface of the spherical source, it is necessary to account for the pressure loss due to flow in the cylinder of soil encased within the infiltrometer. This loss is represented with Darcy's law, for which the flux along the cylinder of soil is

$$q = -K_{fs} \frac{d\Phi}{dz} = -K_{fs} \left(\frac{dP}{dz} + 1 \right) \quad [5a]$$

where Φ is the total potential within the cylinder of soil, and z is the coordinate along the length of the cylinder, positive upward with the origin at the soil surface. This flux is also known from the rate of drop in the water level in the infiltrometer reservoir, that is,

$$q = -\frac{dH(t)}{dt} \quad [5b]$$

Equating these two and integrating with z, the pressure at the spherical source is

$$P(t) = H(t) + L_{max} - \frac{L_{max}}{K_{fs}} \frac{dH(t)}{dt} \quad [5c]$$

Equation [5c] is altered from Philip's analysis to account for the one-dimensional movement of water through the distance L_{max} of the MPD infiltrometer and to account for the geometry of the capped sphere of wetted soil. The total pressure-capillarity potential drop from the spherical source to the wetted front can thus be described by

$$\Delta P = \psi - H(t) - L_{max} + \frac{L_{max}}{K_{fs}} \frac{dH(t)}{dt} \quad [6]$$

where ψ is the Green–Ampt wetting-front suction for the unsaturated soil. The Green–Ampt wetting-front suction is defined as

$$\psi = \int_{h_i}^{0} \frac{K(h)}{K_{fs}} dh \quad [7]$$

where h_i is the initial pressure head and $K(h)$ is the unsaturated hydraulic conductivity, which is a function of the pressure head h.

By equating Eq. [4] and [6], we get the following two equations that can be used to simulate the temporal variations in the ponding depth in the infiltrometer for a given combination of the infiltrometer geometry and soil properties (K_{fs} and ψ):

$$dH = \frac{K_{fs}}{L_{max}} \left\{ \beta \left[(\theta_s - \theta_i) \frac{R^2(t) + R(t)L_{max}}{K_{fs}} \frac{dR}{dt} B - G \right] - \psi + H(t) + L_{max} \right\} dt \quad [8]$$

$$dt = \frac{\beta(\theta_s - \theta_i)\left\{ \left[R^2(t) + R(t)L_{max} \right] / (K_{fs}L_{max}) \right\} B\, dR - \left[(L_{max}/K_{fs})\Delta H \right]}{\psi - H(t) - L_{max} + \left[\beta \left(2r_o^2/L_{max} \right) B \right]} \quad [9]$$

Equations [8] and [9] are just different rearrangements of the equation resulting from equating Eq. [4] and [6], and each can be used in a numerical scheme to optimize for K_{fs} and ψ given a time series of ponding depth measurements. Equations [8] and [9] are discretized in an implicit formulation along H and t, respectively, to facilitate the calculation of measurements of head at given times or the calculation of time at given heads. The discretized forms of the equations are

$$H^n - H^{n-1} = \frac{K_{fs}}{L_{max}} \left(\beta \left\{ (\theta_s - \theta_i) \frac{\left[R^2(t) \right]^n + R^n(t)L_{max}}{K_{fs}} \left(\frac{R^n - R^{n-1}}{\Delta t} \right) B^n - G \right\} - \psi + H^{n-1} + L_{max} \right) \Delta t \quad [10]$$

$$t^n - t^{n-1} = \frac{\beta(\theta_s - \theta_i) \left(\left\{ \left[R^2(t) \right]^n + R^n(t)L_{max} \right\} / K_{fs}L_{max} \right) B^n \left(R^n - R^{n-1} \right)}{\psi - H^n - L_{max} + \left[\beta \left(2r_o^2/L_{max} \right) B^n \right]} - \frac{(L_{max}/K_{fs})\Delta H}{\psi - H^n - L_{max} + \left[\beta \left(2r_o^2/L_{max} \right) B^n \right]} \quad [11]$$

where n and $n-1$ represent the present and previous time steps, respectively, Δt is the time increment, and ΔH is the difference between the previous and present water levels. In the computational procedure, $R(t)$ in Eq. [10] and [11] is computed using Eq. [2] and the measured head in the infiltrometer vs. time data. Equations [10] and [11] can each be applied to simulate observed time series of ponding depth vs. time data and do this in an iterative manner to find the optimum combination of K_{fs} and ψ that yields the best agreement between the observed and simulated ponding depth time series.

The formulation leading to Eq. [8] and [9] is based on the approach presented by Philip (1993) in which it was assumed that the flow from the infiltrometer is driven by a combination of pressure (H) and capillarity (ψ), perturbed by a symmetric gravity flow. The symmetry of the gravity flow does not mean that the gravity component is zero. It is zero at the beginning but then approaches the full downward gravity flow described above [$2\beta r_o^2 \ln(1 + L_{max}/r_o)$]. This type of behavior is well known from infiltration theory (Philip, 1969). With that explanation, we point out that Cheng et al. (2011) presented a formulation of the MPD method, which they referred to as the modified Nestingen (MN) method because they derived their analysis starting from the work of Nestingen (2007). In deriving their cumulative infiltration equation, they did not use the Philip (1993) formulation with the perturbed flow, but rather they accounted for gravity flow by adding constant flow given by $K_{fs}(t - t_o)$, where t_o is the time at which the wetting front reaches the base of the infiltrometer tube and the three-dimensional flow begins. The addition of this term is not consistent with the original Philip (1993) formulation based on the Green–Ampt equation. The effect of incorporating gravity in such an ad hoc manner on the accuracy of their resulting formulation remains to be determined. They also stated that the mass balance equation for the Nestingen formulation neglected the volume of water infiltrated into the encased cylindrical soil section, given by $L_{max}\Delta\theta$. This claim is not correct, though, because that volume of water is fully accounted for in our equation for the capped sphere.

Materials and Methods

To determine the accuracy of the derived equations for the MPD infiltrometer, falling-head data were generated by solving the axisymmetric form of the Richards equation for a series of simulated infiltration experiments for different soils. The MPD infiltrometer Eq. [2], [10], and [11] were then applied to estimate the hydraulic properties of the soils from the simulated falling-head data. Comparison of the soil hydraulic parameters used in the Richards equation simulations with the optimized parameters from the fitting with Eq. [2], [10], and [11] was then used to assess the accuracy of the MPD analysis. The validity of the MPD device and associated analysis was assessed using laboratory experiments involving three large barrels packed with different types of sand.

Numerical Simulations

A numerical solution of Richards' equation was used to provide the falling-head data for evaluation of the analytical method described above. Because the hydraulic parameters are inputs to the numerical solution, there is an exact way of assessing the accuracy of the approximate method. In this study, Richards' equation was solved with the commercial finite element equation solver contained within the COMSOL Multiphysics software package (COMSOL, 2013). One comparison of the MPD infiltrometer with the Philip–Dunne borehole permeameter was conducted to illustrate some differences in response between the two, but most of the analysis focused on the MPD configuration.

Boundary Conditions

Constraints on the solution of Richards' equation are the initial condition, which is initial pressure or initial saturation, and boundary conditions, either specified pressure or specified flux. For the borehole (Philip–Dunne borehole permeameter) domain illustrated in Fig. 3a, the initial condition is one of uniform initial pressure, and the boundary conditions for the individual boundary segments are given by the following:

AB: h = water depth(t) inside the permeameter

BC, CD: $\partial(h + z)/\partial n$

DE: h_i = initial soil water pressure

EF: $\partial(h + z)/\partial n = -1$

AF = $\partial(h + z)/\partial r = 0$ due to axial symmetry

where n is the unit normal vector to the boundary, and r and z represent radial and vertical direction, respectively. For the infiltrometer (MPD infiltrometer) domain illustrated in Fig. 3b, the initial conditions are the same as for the borehole

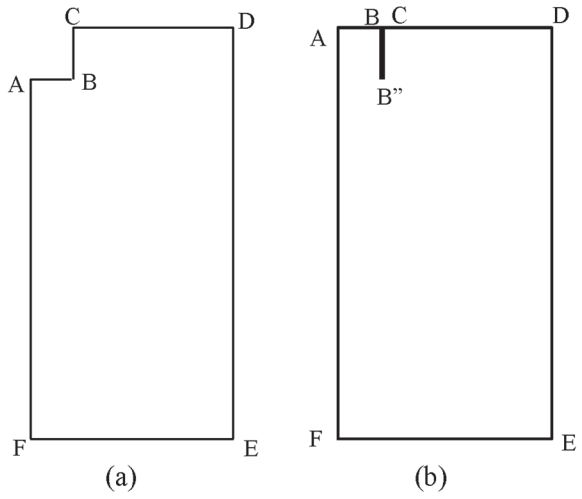

Fig. 3. Illustrations of the axisymmetric domain for (a) the Philip–Dunne permeameter and (b) the modified Philip–Dunne (MPD) infiltrometer.

domain. The boundary conditions for the infiltrometer domain are the following:

AB: h = water depth(t) inside the infiltrometer

BB″ = B″C = CD: $\partial(h + z)/\partial n = 0$

DE: h_i = initial soil water pressure

EF: $\partial(h + z)/\partial n = -1$

AF: $\partial(h + z)/\partial r = 0$ due to axial symmetry

For the two domains, the condition for Boundary EF is for the assumption that a unit hydraulic gradient exists at the bottom boundary. The conditions for Boundaries DE and EF are sufficient as long as the wetting front does not reach the boundaries during the infiltration event. Details concerning the solution domain and the COMSOL solver are presented in the supplemental material.

Description of Input Parameters

For the numerical simulations, five types of soil that are among the most common types found in infiltration practices were chosen. The soil types are loamy sand, sandy clay loam, silt loam, sandy clay, and silty clay. The hydraulic properties of the soils were defined in terms of van Genuchten (1980) parameters. The value of H_i was kept constant at 0.43 m for all numerical simulations, while the hydraulic properties of the soil included the field saturated volumetric soil moisture content θ_s, saturated hydraulic conductivity K_{sat}, and the van Genuchten parameters α and n were within one standard deviation of their respective mean values for the five soil types as described by Carsel and Parrish (1988). In these simulations, the initial soil water pressure was set to yield moderate to full wetting front potential, as calculated from Eq. [7], for each type of soil, while $\Delta\theta$ was limited to relatively small for the finest soil (silty clay) because, in the numerical simulations for fine soil, a very low soil water pressure needs to be set for high $\Delta\theta$ (dry condition), which sometimes can lead to making the numerical simulations difficult to complete due to nonconvergence of solutions.

Another set of simulations was also performed with the solution to the Richards equation for the case where n was kept constant at 4.0 while α and K_{sat} were varied using linear scaling theory (Vogel et al., 1991). According to this theory, the value of α varies in direct proportion to the scaling factor γ: $\alpha = \alpha_{ref}\gamma$, while the value of K_{sat} varies with γ^2: $K_{sat} = K_{sat\_ref}\gamma^2$, where $\alpha_{ref} = 4$ and $K_{sat\_ref} = 1.65 \times 10^{-4}$ m/s are the reference values of α and K_{sat}, respectively. The initial water depth inside the infiltrometer was the same as in the previous simulations, but the initial moisture content and saturated moisture content were set to be 0.055 and 0.375, respectively, thus making $\Delta\theta$ equal to 0.32 for all cases.

The procedure for each simulation was as follows for all of the soils described above. A set of values for θ_s, θ_r, α, K_{sat}, and h_i was defined (Tables 1 and 2) for use as inputs to the COMSOL-MP solver. Richards' equation (Richards, 1931) was then solved for the period when the water level in the MPD infiltrometer was above zero. Using the head vs. time curve produced by the simulation, the defined change in moisture, and the geometry of the infiltrometer, the modified analytical equations were tested using the MPD analysis procedure described above to produce values of K_{fs} and ψ. These parameters were then compared with the values used as inputs for the simulation. The K_{sat} values used as input for the simulation and the K_{fs} values determined from the MPD analysis are termed K_{eff} and K_{MPD}, respectively. The value of ψ determined using the selected values for the van Genuchten parameters in Eq. [7] and determined from the MPD analysis are termed ψ_{eff} and ψ_{MPD}, respectively; ψ_{eff} is determined by applying Eq. [7].

Analysis Procedure

A computational spreadsheet procedure in MS Excel with the Solver add-in and Visual Basic application was developed to find solutions to Eq. [2], [10], and [11] and obtain optimal values of K_{fs} and ψ. The general procedure for finding values of K_{fs} and ψ from the head vs. time data is as follows:

1. Input all variables, including initial moisture content, field saturated moisture content, initial height, and the head vs. time curve.

2. For each measurement of head, use the relationship in Eq. [2] to find the corresponding distance of the sharp wetting front (note: Solver in Microsoft Excel 2010 and a macro were used to automate this step).

3. Estimate the change in head with respect to time and the change in wetting front distance with respect to time by using the forward finite difference method for all values of $R(t)$ equal to or greater than the distance $\sqrt{(r_1^2 + L_{max}^2)}$.

4. Make initial guesses for the values of K_{fs} and ψ. By default, the initial guess for K_{fs} and ψ are set as 1×10^{-3} cm/s and 100 cm, respectively. We found that for a finer soil that has a K_{fs} value of $<1 \times 10^{-5}$ cm/s, the initial guess of ψ might need to be changed to improve the convergence rate.

5. Solve Eq. [10] and [11] for ΔH and Δt at each incremental value of $R(t)$.

6. Minimize the absolute differences between ΔH found in Step 5 and change in the measured head and between Δt and the measured time interval by iterating the values of K_{fs} and ψ. Between these two optimization procedures (ΔH and Δt), the one with the minimum RMSE between measured and estimated data was chosen to calculate K_{fs} and ψ. Occasionally, one of the two does not converge, which is the primary reason that the dual fitting procedure is recommended.

Experiments

Experiment Setup

Three barrels with a diameter of 0.56 m, height of 0.91 m, and volume of 0.208 m^3 (Greif, Inc.) were chosen as vessels for the calibration media. Each barrel was fitted with a threaded polyvinyl chloride valve along the side near the bottom that allowed the water to drain. A thin coating of sand was attached to the

Table 1. Comparison of field-saturated hydraulic conductivity (K_{fs}) and Green–Ampt wetting-front suction (ψ) values determined from the modified Philip–Dunne (MPD) analysis of the simulated falling-head data with the values used as inputs to the COMSOL simulations for the case of variable n (K_{eff} and ψ_{eff}, respectively) and the initial soil water pressure in the numerical simulations (h_i), residual and initial soil moisture content (θ_r and θ_i, respectively), and van Genuchten parameters α and n. The pressure parameter h_s in the Vogel et al. (2000) modified van Genuchten equations was set to −0.04 m for all simulations shown here.

Soil type	α	n	h_i	θ_r	θ_i	K_{MPD}	K_{eff}	K_{MPD}/K_{eff}	ψ_{MPD}	ψ_{eff}	ψ_{MPD}/ψ_{eff}
	m^{-1}		m	%		m/s			m		
Loamy sand	10	2.3	−0.4	5.7	11.8	4×10^{-5}	3.47×10^{-5}	1.15	0.11	0.061	1.84
Sandy clay loam	4.5	1.5	−0.8	10	25	8.66×10^{-6}	6.94×10^{-6}	1.25	0.144	0.097	1.48
Silt loam	2	1.4	−2	6.7	28	1.69×10^{-6}	1.39×10^{-6}	1.22	0.197	0.173	1.13
Sandy clay	0.9	1.2	−10	10	27.9	3.79×10^{-7}	2.78×10^{-7}	1.36	0.26	0.28	0.94
Silty clay	0.4	1.1	−10	7	31.8	6.12×10^{-8}	5.56×10^{-8}	1.10	0.52	0.43	1.21

Table 2. Comparison of field saturated hydraulic conductivity (K_{fs}) and Green–Ampt wetting-front suction (ψ) values determined from the modified Philip–Dunne (MPD) analysis of the simulated falling head data with the values used as inputs to the COMSOL simulations for the case of constant n (K_{eff} and ψ_{eff}, respectively) and the initial soil water pressure in the numerical simulations (h_i), residual and initial soil moisture content (θ_r and θ_i, respectively), and van Genuchten parameters α and n. The parameters α and K_{eff} were derived from linear scaling theory (Vogel et al., 1991), with Case 2 being the reference condition.

Case	α	n	h_i	θ_r	θ_i	K_{MPD}	K_{eff}	K_{MPD}/K_{eff}	ψ_{MPD}	ψ_{eff}	ψ_{MPD}/ψ_{eff}
	m^{-1}		m	%		m/s			m		
1	8	4	−0.50	5	5.5	6.63×10^{-4}	6.60×10^{-4}	1.00	0.14	0.087	1.57
2	4	4	−1	5	5.5	1.63×10^{-4}	1.65×10^{-4}	0.99	0.22	0.17	1.29
3	3	4	−1.33	5	5.5	9.15×10^{-5}	9.28×10^{-5}	0.99	0.28	0.23	1.19
4	2	4	−2	5	5.5	4.11×10^{-5}	4.12×10^{-5}	1.00	0.38	0.35	1.09
5	1.05	4	−3.82	5	5.5	1.07×10^{-5}	1.14×10^{-5}	0.94	0.73	0.66	1.10
6	0.61	4	−6.59	5	5.5	3.84×10^{-6}	3.84×10^{-6}	1.00	1.13	1.14	0.99
7	0.40	4	−10	5	5.5	1.64×10^{-6}	1.65×10^{-6}	0.99	1.71	1.74	0.98
8	0.27	4	−14.93	5	5.5	7.79×10^{-7}	7.52×10^{-7}	1.04	2.4	2.57	0.93
9	0.17	4	−23.57	5	5.5	4×10^{-7}	2.98×10^{-7}	1.34	2.87	4.09	0.70

inner walls of the barrels with a spray adhesive to roughen the surface and minimize the potential for preferential flow of water along the walls. A 0.076-m layer of pea gravel (median diameter = 0.006 m) was placed at the bottom of the barrel and covered with a coarse filter fabric to isolate the gravel from the medium above. Sand media of three particle size distributions were added to the three barrels over the filter fabric to a height of 0.51 m, stopping (roughly) every 0.05 m to tamp down the sand to prevent large voids and non-uniform compaction.

The three sand media used in the experimental testing were: (i) 100% ASTM C-33 sand (Barrel 1), (ii) 80% (w/w) ASTM C-33 sand with 20% US Silica F110 sand (Barrel 2), and (iii) 100% US Silica F110 sand (Barrel 3). The media were selected to represent a range of relatively high permeability engineered soils used in bioretention facilities and other infiltration practices. For example, Winogradoff (2002) recommends using 50 to 60% clean ASTM C-33 construction sand with 20 to 30% sandy loam or loamy sand and 20 to 30% leaf compost material for a soil medium. Other manuals recommend similar mixes. The compost was omitted from our media to achieve homogeneous mixtures that would not change with time due to dissolution or degradation of the organic material. The sand media were mixed in a portable mortar mixer before addition to the barrels. The particle size distribution for each sand mixture was determined by a sieve analysis (ASTM, 2006) and is given in Fig. 4.

Modified Philip–Dunne Infiltrometer Tests

The MPD infiltrometer was inserted 5 cm into the surface of the soil near the center of the barrel. Initial soil moisture measurements were made from five locations around the outside edge of the infiltrometer at the soil surface. The initial soil moisture content was assumed to be uniform for the whole media. These measurements were made either gravimetrically (Gardner, 1986; ASTM, 2000, 2005) or with a calibrated moisture probe (Theta Probe ML2x). The temperature of the water used to fill the infiltrometer was measured. The MPD infiltrometer was then filled to a height of 0.43 m with the water. The head of water with time

during the test was recorded at a rate of six readings per minute with an ultrasonic sensor (MassaSonic M-5000) mounted above the device. Immediately after the water had completely drained from the infiltrometer tube, the infiltrometer was removed from the barrel and five final moisture content measurements were made. Eleven, 17, and 19 independent tests were conducted with the MPD infiltrometer on Barrels 1, 2, and 3, respectively.

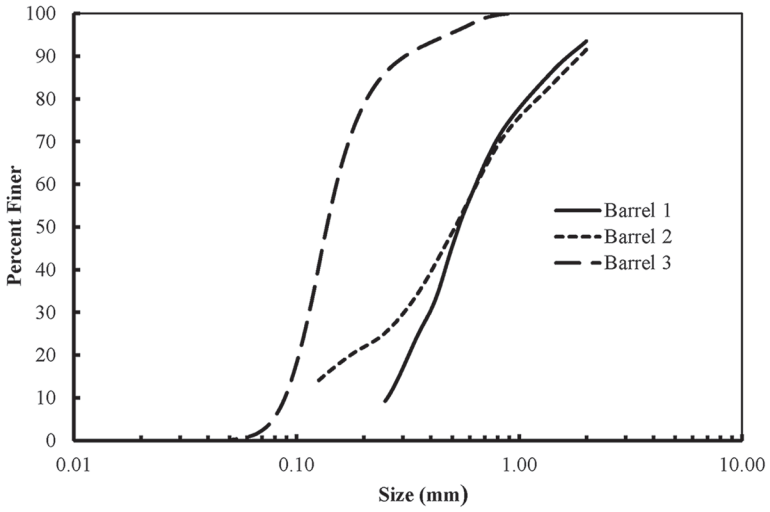

Fig. 4. Particle size distributions of the three media used for infiltration testing.

Reference Falling-Head Tests

To perform a reference falling-head test, the barrel was filled at an approximate flow rate of 0.005 L/s from a hose connected to a valve opened into the pea gravel layer at the bottom of the barrel. This method of filling the barrels from the bottom up at low flow was used to minimize the amount of entrapped air in the soil voids. The flow rate during filling was maintained below that required to fluidize the sand so as not to disturb the bed. When the water level was approximately 0.2 m above the sand surface, the valve was closed and the hose was disconnected. An ultrasonic sensor was then mounted to the top of the barrel. The valve at the bottom was opened and the head vs. time data were recorded. The analysis for the reference falling-head test was similar to the analysis of a falling-head laboratory permeameter. In the case of a falling head, the flow and hydraulic gradient are both time dependent. Darcy's law (Klute and Dirksen, 1986) is used to calculate the saturated hydraulic conductivity K_{sat} according to

$$K_{sat} = \frac{L}{\Delta t}\left(\frac{T_i + L}{T_{i+1} + L}\right) \quad [12]$$

where L is the length of the soil column, and T_i and T_{i+1} are ponded-head depths at the beginning and end of the time interval Δt. The barrels were conditioned for these tests by performing filling and draining in the same manner as described above approximately seven times before beginning the reference falling-head tests. Twenty-five, 20, and 21 reference falling-head tests were performed on Barrels 1, 2, and 3, respectively.

Reference Falling-Head Tests vs. Modified Philip–Dunne Infiltrometer

The mean K_{fs} for each medium determined by the MPD infiltrometer using the MPD analysis procedure ($\overline{K}_{MPD}$) was compared with the mean K_{sat} of the reference falling-head tests for the same medium ($\overline{K}_{ref}$). The uncertainty, U_r, of the ratio $K_R = \overline{K}_{MPD} / \overline{K}_{ref}$ is defined by following the ASME standard technique (Abernethy et al., 1985):

$$U_R = \sqrt{\left(\frac{\partial K_R}{\partial \overline{K}_{MPD}} U_{K\_MPD}\right)^2 + \left(\frac{\partial K_R}{\partial \overline{K}_{ref}} U_{K\_ref}\right)^2}$$
$$= \sqrt{\left(\frac{1}{\overline{K}_{ref}} U_{K\_MPD}\right)^2 + \left(\frac{\overline{K}_{MPD}}{\overline{K}_{ref}^2} U_{K\_ref}\right)^2} \quad [13]$$

where U_{K_MPD} is the uncertainty of the K_{fs} value determined by the MPD analysis for each medium, U_{K_ref} is the uncertainty of the K_{sat} value determined by reference falling-head analysis for each medium, $\overline{K}_{MPD}$ is the mean value of K_{fs} determined by the MPD analysis for each medium, and $\overline{K}_{ref}$ is the mean value of K_{sat} determined by the reference falling-head analysis for each medium. The values of U_{K_MPD} and U_{K_ref} are determined by

$$U_{K\_MPD} = t_s \frac{\sigma_{K\_MPD}}{\sqrt{N_{MPD}}}$$

and

$$U_{K\_ref} = t_s \frac{\sigma_{K\_ref}}{\sqrt{N_{ref}}}$$

where σ_{K_MPD} and σ_{K_ref} represent the standard deviation of MPD measurements and reference falling-head measurements, respectively, t_s is the Student's t value, and N_{MPD} and N_{ref} represent the number of measurements for MPD analysis and reference falling-head analysis, respectively.

Results and Discussion

Richards' Equation Simulations

Borehole Permeameter vs. Modified Philip–Dunne Infiltrometer

It is instructive to compare computer simulations of infiltration into a homogeneous and isotropic soil for the two cases, one for the Philip-Dunne permeameter and one for the MPD infiltrometer, just to show the differences in infiltration characteristics. For this, a soil with the following soil moisture characteristics was used: $\theta_s = 0.375$, $\theta_r = 0.05$, $\alpha = 4\ m^{-1}$, $n = 4$, and $K_{sat} = 1.64 \times 10^{-4}$ m/s. The initial water pressure was set to −1.0 m, which gives a

corresponding initial moisture content of 0.055. The simulation result for a 0.05-m-deep, 0.05-m-radius borehole (Philip–Dunne permeameter) is shown in Fig. 5. The results for the MPD infiltrometer with a 0.05-m radius penetrated to the 0.05-m depth are shown in Fig. 6. Both plots show the moisture distribution in the soil surrounding the infiltration surface at the moment that the ponding in the tube becomes zero. There are some similarities in the geometry of the flow for both cases, but there are also some differences. Primarily, the water in the MPD infiltrometer is forced to pass one-dimensionally through the 0.05-m-long soil core before allowing for three-dimensional flow in the soil beneath and around the infiltrometer. This flow constraint for the MPD infiltrometer results in a reduced water pressure at the end of the tube compared with a Philip–Dunne permeameter due to the pressure loss within the soil core, and this then results in a longer time for the infiltrometer tube to empty and a more diffusive wetting front than for the permeameter.

To illustrate the effect of borehole depth and infiltrometer penetration depth on the time variation of water height inside the permeameter and infiltrometer tubes, simulations for a few different penetration depths were conducted using Richards' equation for the same initial condition as described above; the results of these are presented in Fig. 7. It can be observed from the plots that the borehole depth for the permeameter does not affect the rate of water height decrease for borehole depths in the range between 0.15 and 0.05 m. The depth of the borehole does begin to influence the infiltration rate at 0.02 m and even more so for surface application. This influence of borehole depth results from the fact that when the wetting front reaches the soil surface, which it would do for the shallower boreholes, the rate of infiltration is restricted because there is less volume of soil to be invaded by the advancing front.

Infiltration rates for the MPD infiltrometer configuration are much slower than for the permeameter at equivalent borehole or penetration depths. Also, it can be observed that the time required for emptying of the initially filled volume for the case with a 0.05-m tube penetration is more than twice the time required for the case of surface application and about 30% more time than for the case of 0.02-m penetration. This results from the pressure loss that occurs in transmitting the water through the encased soil volume as opposed to an open borehole.

Simulations of the Modified Philip–Dunne Infiltrometer for Various Soils

The input parameters for the soils where the value of the van Genuchten parameters (α and n) were reported by Carsel and Parrish (1988) for the five soil textures of loamy sand, sandy clay loam, silt loam, sandy clay, and silty clay are presented in Table 1, along with the corresponding K_{fs} and ψ values estimated from the MPD analysis procedure for each texture. The input parameters for the soils with parameters derived from linear scaling theory are

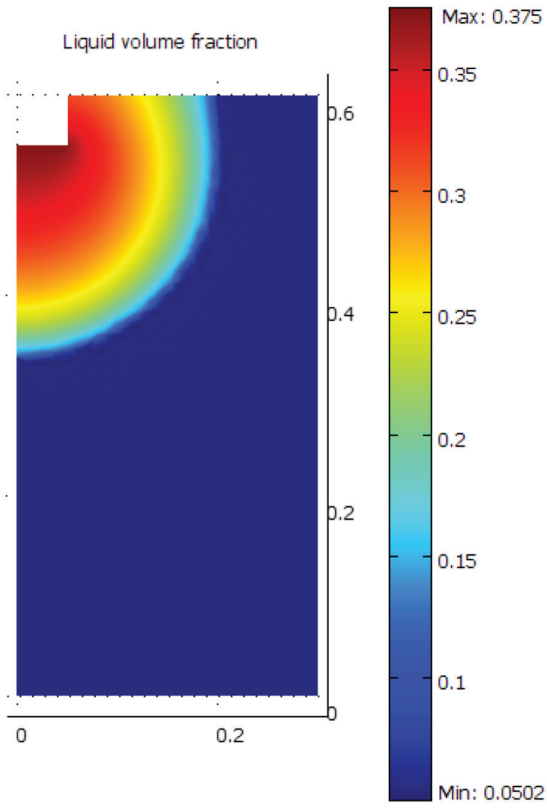

Fig. 5. Soil moisture content at 380 s for the Philip–Dunne permeameter at the end of the simulation period when the permeameter tube has emptied.

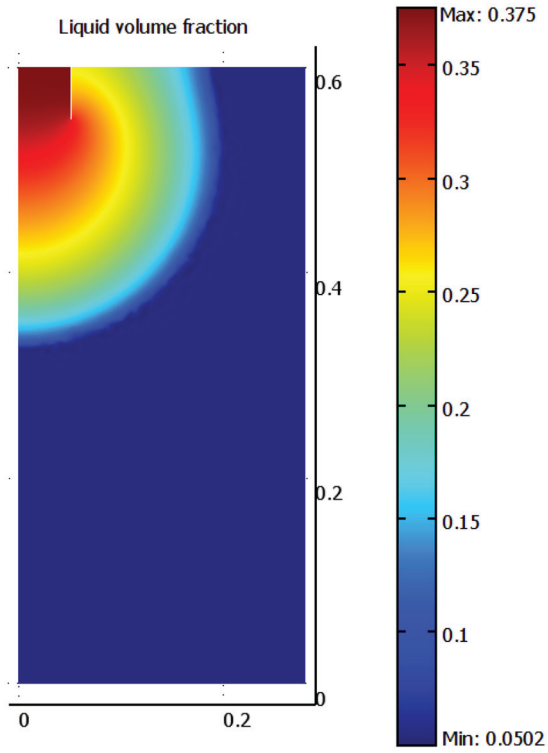

Fig. 6. Soil moisture content at 1200 s for the modified Philip–Dunne infiltrometer at the end of the simulation period when the infiltrometer tube has emptied.

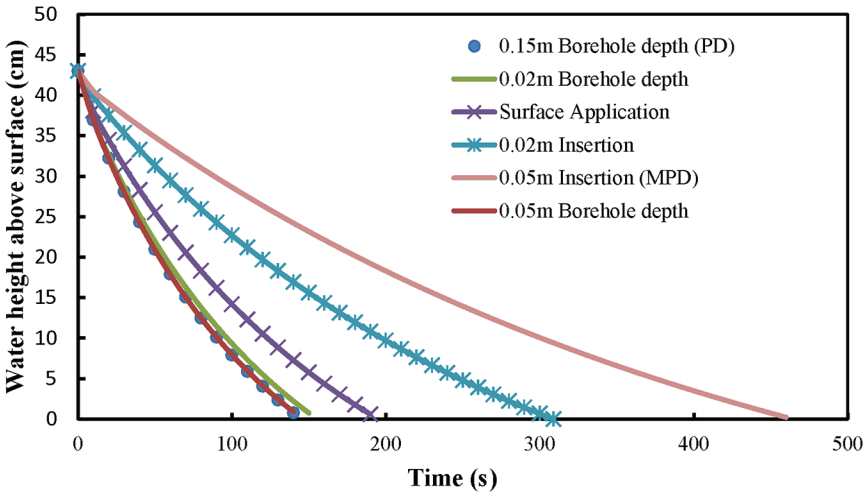

Fig. 7. Water depth in the Philip-Dunne (PD) permeameter or modified Philip–Dunne (MPD) infiltrometer vs. time. Initial water depth = 0.43 m.

presented in Table 2, and again the K_{fs} and ψ values estimated from the MPD analysis procedure corresponding to each soil are also given in Table 2. Note that all the soils with the scaled parameters had the parameter n set equal to 4. The K_{sat} values that were input in the numerical simulations are termed K_{eff} for both Tables 1 and 2.

According to the results in Table 1 and Fig. 8, the MPD analysis procedure overestimated K_{fs} by 10% (silty clay, $\alpha = 0.4$, $n = 1.1$) to 36% (sandy clay, $\alpha = 0.9$, $n = 1.2$) for the soil cases examined. The variation of the K_{MPD}/K_{eff} ratio with α is shown in Fig. 8. Part of the overestimation of K_{fs} is believed to be due to the distortion of the actual flow path lines caused by the no-flow boundaries of the infiltrometer. This distortion effect should be accounted for in the value of β, and the distortion should increase with increasing capillarity. It is not clear that the constant value of β as assigned by Philip (1993) is correct or whether it would be better to assign a value of

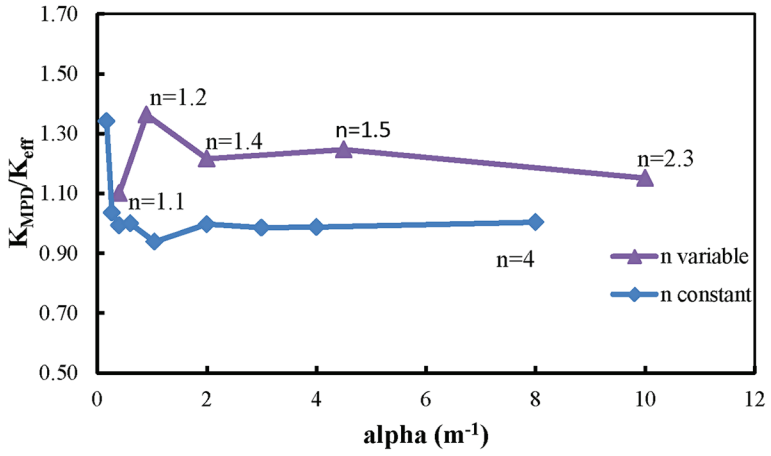

Fig. 8. Variation of the ratio of the field-saturated hydraulic conductivity estimated from the modified Philip–Dunne (MPD) analysis procedure with the saturated hydraulic conductivity values input in the numerical simulations (K_{MPD}/K_{eff}) for different values of the van Genuchten parameters α and (variable or constant) n.

β that accounts for capillarity. This effect should be examined further.

Reynolds (2011) used an ad hoc modified version of HYDRUS-2D to show that using $\beta = \pi^2/8$ in the Philip–Dunne permeameter analysis leads to overestimation of the K_{fs} ranging from a few percentage points to about 23% for the different soils he examined. For the borehole permeameter, he suggested this coefficient to be 1. In his analysis using $\beta = 1$, the measured K_{fs} value was consistently more accurate ($\leq$20% difference).

A second possible reason for the overestimated K_{fs} value is that the MPD analysis assumes that the wetting front is sharp. In the field, however, and also in simulations of Richards' equation, the wetting front is not sharp but will be diffuse to a degree determined by the capillarity of the soil. According to the results in Table 2 and Fig. 8, where n was kept constant, the MPD analysis procedure in some cases overestimated K_{fs} (Case 9, 34%) and in some cases underestimated K_{fs} (Case 5, 6%). Overall in these cases, however, the MPD analysis predicted K_{fs} better than the cases where n was variable (Table 1). The reason is probably because a higher n value, such as $n = 4$, represents a narrower particle size distribution and a less diffuse wetting front, which corresponds more closely to the assumption of a sharp wetting front made in the Green–Ampt analysis.

From Tables 1 and 2 we can also conclude that the MPD formulation overestimated ψ in some cases (84% for loamy sand and 57% for Case 1) and underestimated it in other cases (6% for sandy clay and 30% for Case 9). A similar kind of trend, going from coarser textured materials to finer textured materials, was shown by Reynolds (2011) for the borehole permeameter. He noted that this inaccuracy seems to be associated with the gravity term G in the Green–Ampt solution formulation, which was kept constant during the entire period of infiltration in his analysis and in the analysis of Philip (1993). The gravity term was kept constant in those two analyses because in both cases the governing equation was integrated analytically with time, which required that the gravity term be constant. In contrast, in our analysis, the gravity term was not kept constant because we integrated the governing equation (Eq. [8] or [9]) numerically, allowing the flexibility of a time-variant gravity term. Reynolds (2011) found that the detrimental effect of a constant gravity term on the estimated ψ is greatest for coarser soils and demonstrated that a constant value of zero (rather than r_o) leads to improved estimates of the wetting front suction for the entire range of soil textures.

Another assumption made in the MPD formulation is that the wetting front will be hemispherical in shape. In reality, however, because of the effect of gravity, the wetting front cannot be perfectly hemispherical after some period of infiltration. It will be more elongated in shape (i.e., bulged downward). This elongation may be another cause of deviation of parameter estimates from the input values. To illustrate this effect, the moment of inertia about the axis of symmetry was calculated for each of the Richards' equation solutions. The moment of inertia (M) about the axis of symmetry is one way to quantitatively represent the shape of the wetting front. It was calculated as a function of time using

$$M(t) = \int_o^t 2\pi\theta(t) r^2 \mathrm{d}r\mathrm{d}z \qquad [14]$$

Simulations of Richards' equation were performed with and without the presence of gravity for each type of soil and the values of M were calculated from Eq. [14] for the instant in time at which the infiltrometer just emptied. Results for these integrations are listed in Table 3, where the moment of inertia for cases without gravity (M_C) are given as a ratio with the moment of inertia for the cases with gravity (M_{C+G}). The amount of elongation depends on the ratio of capillary forces to gravitational forces. From Table 3, it can be seen that the coarser soils (i.e., loamy sand and sandy clay loam) have a larger ratio than the finer soils, indicating the importance of the gravitational component of flow for those soils. It also indicates that the wetting front will not be spherical as assumed in the Green–Ampt analysis, and this could be a cause for some reduction in accuracy of parameter estimates with the MPD analysis.

Table 3. Comparison of the spread of the wetting front at the end of the simulation period, when the infiltrometer tube has emptied, for different types of soil, where K_{eff} is the saturated hydraulic conductivity values that were input in the numerical simulation and M_C and M_{C+G} are the moments of inertia without and with gravity, respectively.

Soil type	K_{eff}	M_C/M_{C+G}
	m/s	
Loamy sand	3.47×10^{-5}	1.36
Sandy clay loam	6.94×10^{-6}	1.08
Silt loam	1.39×10^{-6}	1.01
Sandy clay	2.78×10^{-7}	1.0
Silty clay	5.56×10^{-8}	1.0

Illustration of the elongation of the wetted volume for the case of the loamy sand soil is presented in Fig. 9. Figure 9a shows the

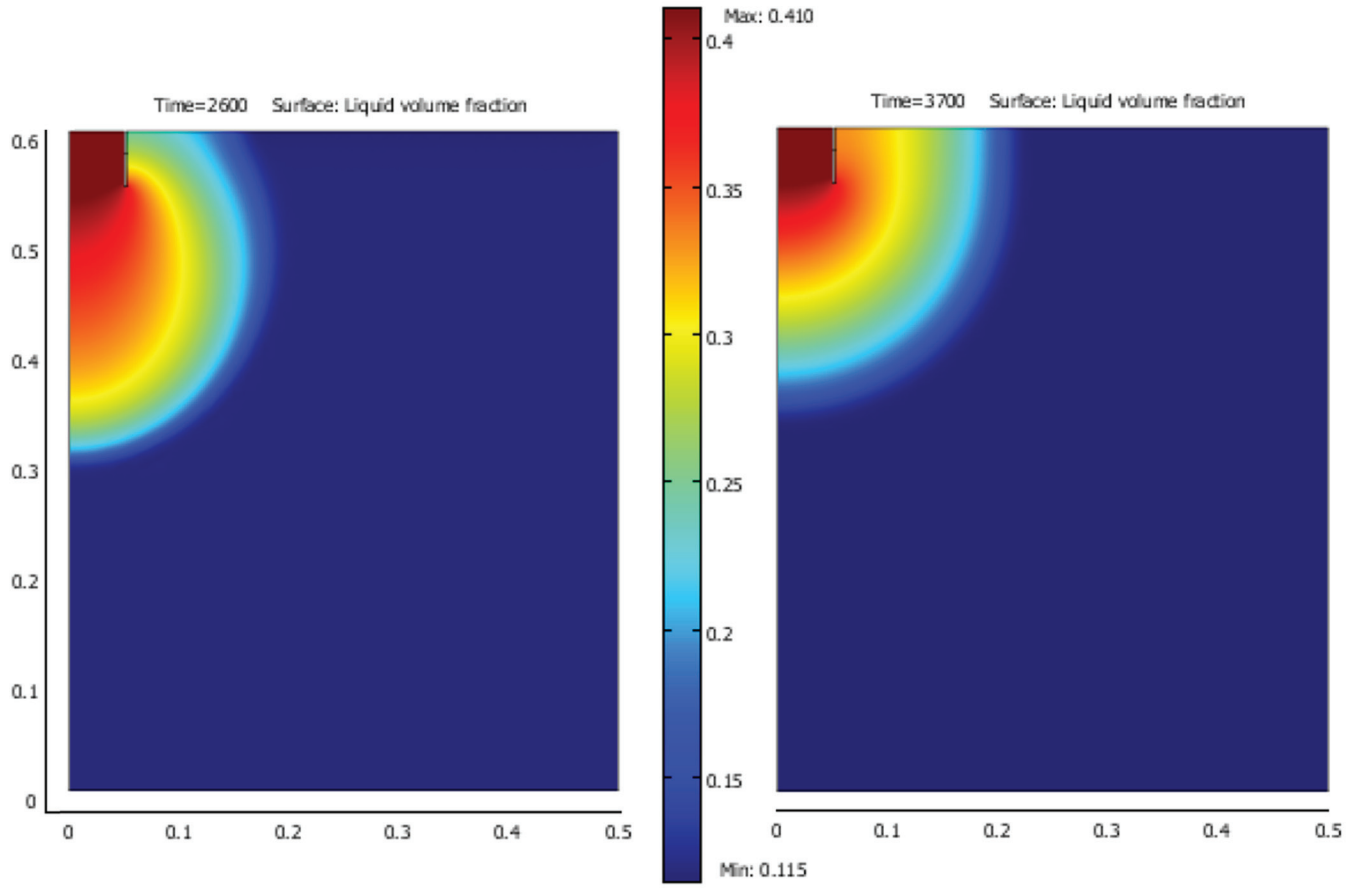

Fig. 9. Illustration of the effect of gravity on downward distortion of the otherwise spherical shaped wetted domain. Loamy sand is compared (a) with gravity and (b) without gravity.

wetted profile for the case with gravity, and Fig. 9b shows the case without gravity. There is a clear effect of gravity in the elongation of the wetting profile in this case.

Experimental Results

Treatment of Outliers

Although the flow rate during filling was maintained below that required to fluidize the sand, in some cases the soil was still slightly fluidized. This led to some unusually high K_{sat} values or outliers, which were not observed when the soil was freshly recompacted. These outliers were removed to obtain a data set free of erroneous measurements caused by experimental error such as equipment malfunctions and operational issues. Outliers were identified (and removed from further consideration) using the median absolute difference method developed by Rousseeuw (1990). The technique incorporates an estimate of scale, S,

$$S = 1.483\left(\text{median}\left|K_i - K_{\text{med}}\right|\right) \quad [15]$$

where K_i is the saturated hydraulic conductivity of the ith test and K_{med} is the median of the K_i values. Then a Z score for each data point is determined from

$$Z_i = \frac{K_i - K_{\text{med}}}{S} \quad [16]$$

Any data that have a Z score above a critical value is considered an outlier. If the distribution is Gaussian, critical Z scores of 2.5 and 1.5 correspond to the inclusion of 98.5 and 84% of the total data, respectively. A histogram of individual K_{ref} and K_{MPD} values (including outliers) of each medium type is shown in Fig. 10. For Media 1 and 2, there is a wider range of K_{ref} values than of K_{MPD} values, and in Medium 3, the variation of K_{MPD} is wider. Because of this wide range of K_{ref} and K_{MPD} values, which leads to difficulty in obtaining representative falling-head tests, a low Z value of 1.5 was used to treat the outliers. Approximately 16% of the data was identified as outliers, indicating that the measurements varied from a Gaussian distribution at the extremes. Outlier distribution among the different devices and barrels appeared to be random.

Comparison between Falling-Head Test and Modified Philip–Dunne Test

The ratio of the arithmetic mean of K_{MPD} and the arithmetic mean of K_{ref} (excluding outliers) for the three sands measured with the MPD infiltrometer are presented in Fig. 11, with corresponding descriptive statistics in Table 4. The graph also shows the upper and lower limits of the ratio ($K_{\text{MPD}}/K_{\text{ref}}$) within the 67% confidence interval around the ratio of the mean K_{MPD} and mean K_{ref}. Equation [13] was used to calculate the upper and lower confidence interval of the ratio ($K_{\text{MPD}}/K_{\text{ref}}$) for each barrel.

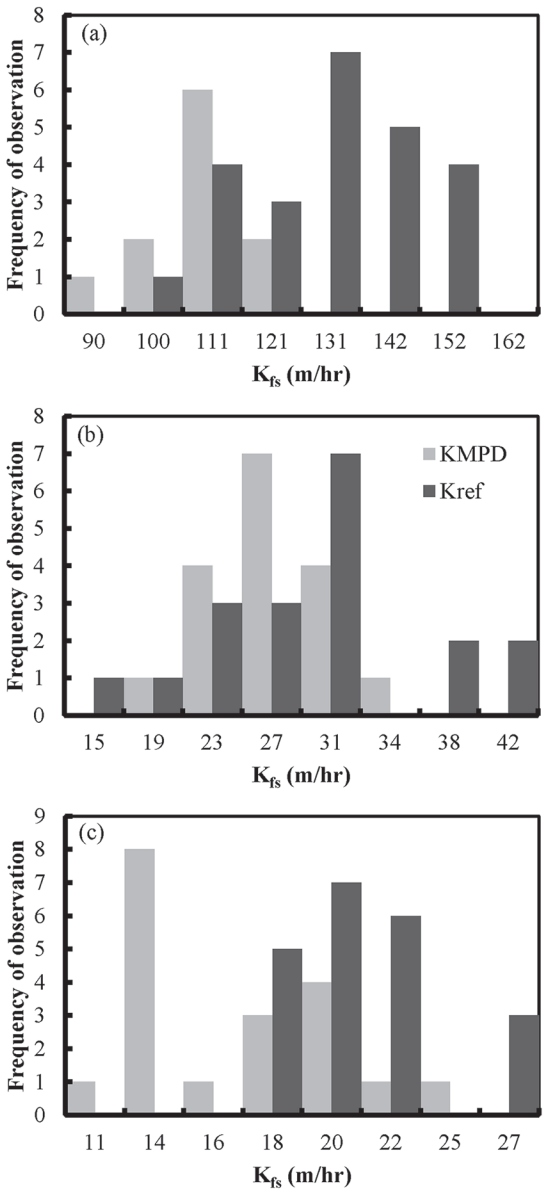

Fig. 10. Histogram of the mean field-saturated hydraulic conductivity value for each medium determined by the modified Philip–Dunne (MPD) infiltrometer (K_{MPD}) and the mean saturated hydraulic conductivity of the reference falling-head tests (K_{ref}) before removing outliers for (a) Medium 1, (b) Medium 2, and (c) Medium 3.

Medium 1 has the highest K_{sat} value and Media 2 and 3 have roughly equivalent K_{sat} values, which are because of the fines present that restrict the passage of water, and the fines are similar in both media. The average initial moisture content for Media 1, 2, and 3 are 6, 10.5, and 7.6%, respectively, for the MPD infiltrometer test. The coefficients of variation (CVs) for all the tests are relatively low, ranging from 4.8 to 21.5%. Muñoz-Carpena et al. (2002) reported CV values of 39 to 101% when comparing permeameter results from field measurements. Asleson et al. (2009) reported CV values between 54 and 178% in an infiltration assessment of rain gardens with engineered soil. Lower CV values would be expected for a controlled laboratory comparison

because the sand medium is homogenous in comparison to field soils. The relatively low skewness and kurtosis values indicate that the data sets may be described as normally distributed. This could also be a consequence of the relatively homogenous sands used in the testing. Comparatively, it is typical for field-measured hydraulic conductivity to be represented by a lognormal distribution (Asleson et al., 2009).

A Games and Howell procedure (Toothaker, 1994) was used to compare the mean K_{sat} values for each of the barrels with the K_{fs} values estimated with the MPD infiltrometer. The results showed that the mean K_{fs} values from the MPD infiltrometer measurements were statistically different at the 5% level from the mean reference falling-head test K_{sat} values for Barrels 1 and 3 but not for Barrel 2. In general, the K_{fs} values from the MPD infiltrometer tests were in good agreement with the reference falling-head tests. Nevertheless, there was a consistent bias in that the mean K_{fs} values were 80, 92, and 78% of the mean reference falling-head tests for Barrels 1, 2, and 3, respectively. One possible reason for this bias is the air entrapment or encapsulation by the downward advancing wetting front during the MPD measurements. The MPD infiltrometer measures the field-saturated hydraulic conductivity (K_{fs}), which will generally be less than that of fully saturated media (K_{sat}). Bouwer (2002) showed that because of entrapped air, the hydraulic conductivity in a wetted zone during infiltration is less than the fully saturated value and indicated that for sandy soil this can cause decreases up to a factor of 2 in the measured K_{fs} value. Given that the barrels were wetted to saturation from the bottom up before the falling-head tests, - much less entrapped air could reasonably be expected in the sands during the falling-head tests and hence a greater saturated hydraulic conductivity value. Fortunately, this amount of bias is relatively low in comparison to the amount of variability observed for MPD infiltrometer measurements at field sites (mean CV of 107%; Asleson et al., 2009).

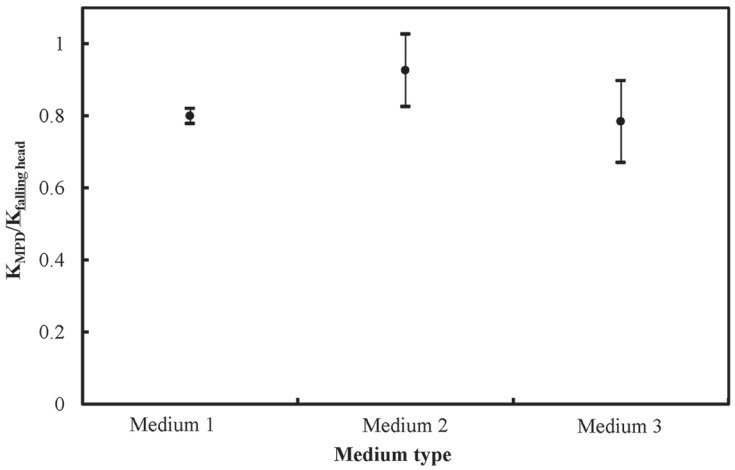

Fig. 11. Comparison of ratio of arithmetic mean of K_{MPD} and arithmetic mean of K_{ref} for three different porous media. Error bars represent 67% confidence intervals.

Conclusions

Infiltration rate parameters, including K_{fs}, should be measured at the soil surface in stormwater infiltration practices because surface issues (e.g., compaction, particle accumulation) can severely limit infiltration and the overall performance of these stormwater management practices. We have developed a novel and inexpensive device for surface infiltration rate measurements, called the modified Philip–Dunne infiltrometer, and an associated approximate data analysis method. Such a device could be used to determine when and where to perform maintenance in stormwater infiltration practices. In addition, this device could also be used for evaluation of landscape-altering practices such as construction activities.

An MPD analysis method was developed based on the Green–Ampt model, which assumes a sharp, spherical wetting front. The

Table 4. Descriptive statistics for the hydraulic conductivity of three barrels of soil media determined by the modified Philip–Dunne infiltrometer and the falling-head method.

	Medium 1		Medium 2		Medium 3	
Statistic	MPD	Falling head	MPD	Falling head	MPD	Falling head
Min., m/s	2.7×10^{-4}	3×10^{-4}	5.8×10^{-5}	5.2×10^{-5}	3.1×10^{-5}	4.7×10^{-5}
Max., m/s	3×10^{-4}	4×10^{-4}	8×10^{-5}	1×10^{-4}	5.6×10^{-5}	6.1×10^{-5}
Mean, m/s	2.9×10^{-4}	3.6×10^{-4}	6.8×10^{-5}	7.4×10^{-5}	4.2×10^{-5}	5.4×10^{-5}
Median, m/s	2.9×10^{-4}	3.6×10^{-4}	6.8×10^{-5}	7.6×10^{-5}	3.9×10^{-5}	5.5×10^{-5}
SD, m/s	1.4×10^{-5}	3.1×10^{-5}	7×10^{-6}	1.4×10^{-5}	9×10^{-6}	4.4×10^{-6}
CV†, %	4.8	8.6	10.5	19.1	21.5	8.2
Skewness	−0.1648	−0.3177	0.31	0.71	0.27	−0.01
Kurtosis	−1.309	−0.7244	−0.85	0.61	−1.72	−1.30
N‡	8	20	15	16	18	18

† Coefficient of variation.
‡ Sample size.

MPD analysis method produced a reasonably accurate estimate of hydraulic conductivity for simulated MPD tests of homogeneous and isotropic soil. The MPD analysis method, however, overestimated the K_{fs} (10–36%) for low n values (n = 1.1–2.3) and overestimated or underestimated (−6 to 34%) for high n values (n = 4), which was attributed to (i) the value of the shape factor proposed by Philip (1993), which does not fully account for possible effects of capillarity on the wetted volume shape, and (ii) the wetting front being neither sharp nor necessarily spherical in shape, both of which are assumptions made with the Green–Ampt analysis. The accuracy of the infiltrometer was tested by comparison with reference falling-head tests on three barrels containing sand media with different grain size distributions. The MPD infiltrometer K_{fs} values were, on average, 83.3% of the reference falling-head test values. The error in K_{fs} values produced by the MPD infiltrometer is thought to be small compared with the orders of magnitude of variability in K_{fs} observed in the field.

References

Abernethy, R.B., R.P. Benedict, and R.B. Dowdell. 1985. ASME measurement uncertainty. J. Fluids Eng. 107:161–164. doi:10.1115/1.3242450

Ahmed, F., J. Gulliver, and J. Nieber. 2011. Rapid infiltration measurement of LID best management practices. In: R.E. Beighley II and M.W. Killgore, editors, Bearing Knowledge for Sustainability: Proceedings of the World Environmental and Water Resources Congress, Palm Springs, CA. 22–26 May 2011. Am. Soc. Civ. Eng., Reston, VA.

Asleson, B.C., R.S. Nestingen, J.S. Gulliver, R.M. Hozalski, and J.L. Nieber. 2009. Assessment of rain gardens by visual inspection and controlled testing. J. Am. Water Resour. Assoc. 45:1019–1031. doi:10.1111/j.1752-1688.2009.00344.x

ASTM. 2000. D 4643-00: Standard test method for determination of water (moisture) content of soil by the microwave oven method. ASTM, West Conshohocken, PA.

ASTM. 2003. D3385-03: Standard test method for infiltration rate of soils in field using double-ring infiltrometer. ASTM, West Conshohocken, PA.

ASTM. 2005. D2216-05: Standard test method for laboratory determination of water (moisture) content of soil and rock by mass. ASTM, West Conshohocken, PA.

ASTM. 2006. C136: Standard test method for sieve analysis of fine and coarse aggregates. ASTM, West Conshohocken, PA.

Bagarello, V., M. Iovino, and D. Elrick. 2004. A simplified falling-head technique for rapid determination of field-saturated hydraulic conductivity. Soil Sci. Soc. Am. J. 68:66–73. doi:10.2136/sssaj2004.6600

Bouwer, H. 2002. Artificial recharge of groundwater: Hydrogeology and engineering. Hydrogeol. J. 10:121–142. doi:10.1007/s10040-001-0182-4

Carsel, R.F., and R.S. Parrish. 1988. Developing joint probability distributions of soil water retention characteristics. Water Resour. Res. 24:755–769. doi:10.1029/WR024i005p00755

Cheng, Q., X. Chen, X. Chen, Z. Zhang, and M. Ling. 2011. Water infiltration underneath single-ring permeameters and hydraulic conductivity determination. J. Hydrol. 398:135–143. doi:10.1016/j.jhydrol.2010.12.017

COMSOL. 2013. COMSOL Multiphysics users guide, Version 3.5a. COMSOL AB, Stockholm.

Gardner, W.H. 1986. Water content. In: A. Klute, editor, Methods of soil analysis. Part 1. Physical and mineralogical methods. 2nd ed. SSSA Book Ser. 5. SSSA and ASA, Madison, WI. p. 493–544. doi:10.2136/sssabookser5.1.2ed.c21

Klute, A., and C. Dirksen. 1986. Hydraulic conductivity and diffusivity: Laboratory methods. In: A. Klute, editor, Methods of soil analysis. Part 1. Physical and mineralogical methods. 2nd ed. SSSA Book Ser. 5. SSSA and ASA, Madison, WI. p. 687–734. doi:10.2136/sssabookser5.1.2ed.c28

Lassabatere, L., R. Angulo-Jaramillo, J.M. Soria Ugalde, R. Cuenca, I. Braud, and R. Haverkamp. 2006. Beerkan estimation of soil transfer parameter through infiltration experiments: BEST. Soil Sci. Soc. Am. J. 70:521–532. doi:10.2136/sssaj2005.0026

Muñoz-Carpena, R., C.M. Regalado, J. Alvarez-Benedi, and F. Bartoli. 2002. Field evaluation of the new Philip–Dunne permeameter for measuring saturated hydraulic conductivity. Soil Sci. 167:9–24. doi:10.1097/00010694-200201000-00002

Nestingen, R.S. 2007. The comparison of infiltration devices and modification of the Philip–Dunne permeameter for the assessment of rain gardens. M.S. thesis. Univ. of Minnesota, Minneapolis.

Nimmo, J.R., K.M. Schmidt, K.S. Perkins, and J.D. Stock, 2009. Rapid Measurement of Field-Saturated Hydraulic Conductivity for Areal Characterization, Vadose Zone J. 8:142–149, doi:10.2136/vzj2007.0159

Olson, N. 2010. Quantifying stormwater infiltration rates on developed soils amended with tillage and compost. M.S. thesis. Univ. of Minnesota, Minneapolis.

Olson, N.C., J.S. Gulliver, J.L. Nieber, and M. Kayhanian. 2013. Remediation to improve infiltration into compact soils. J. Environ. Manage. 117:85–95. doi:10.1016/j.jenvman.2012.10.057

Parr, J.R., and A.R. Bertrand. 1960. Water infiltration into soils. Adv. Agron. 12:311–363. doi:10.1016/S0065-2113(08)60086-3

Philip, J.R. 1969. Theory of infiltration. Adv. Hydrosci 5:215–296. doi:10.1016/B978-1-4831-9936-8.50010-6

Philip, J.R. 1992. Falling head ponded infiltration. Water Resour. Res. 28:2147–2148. doi:10.1029/92WR00704

Philip, J.R. 1993. Approximate analysis of falling-head lined borehole permeameter. Water Resour. Res. 29:3763–3768. doi:10.1029/93WR01688

Reynolds, W.D. 2008. Unsaturated hydraulic properties: Field tension infiltrometer. In: M.R. Carter and E.G. Gregorich, editors, Soil sampling and methods of analysis. 2nd ed. CRC Press, Boca Raton, FL. p. 1107–1127.

Reynolds, W.D. 2011. Measuring soil hydraulic properties using a cased borehole permeameter: Falling-head analysis. Vadose Zone J. 10:999–1015. doi:10.2136/vzj2010.0145

Reynolds, W.D., and D.E. Elrick. 1990. Ponded infiltration from a single ring: I. Analysis of steady flow. Soil Sci. Soc. Am. J. 54:1233–1241. doi:10.2136/sssaj1990.03615995005400050006x

Richards, L.A. 1931. Capillary conduction of liquids through porous mediums. Physics 1:318–333. doi:10.1063/1.1745010

Rousseeuw, P.J. 1990. Robust estimation and identifying outliers. In: H.M. Wadsworth, editor, Handbook of statistical methods for engineers and scientists. McGraw-Hill, New York. p. 16.1–16.24.

Toothaker, L.E. 1994. Multiple comparison procedures. Quant. Appl. Social Sci. Ser. 89. Sage Publ., Newbury Park, CA.

van Genuchten, M.Th. 1980. A closed-form equation for predicting the hydraulic conductivity of unsaturated soils. Soil Sci. Soc. Am. J. 44:892–898. doi:10.2136/sssaj1980.03615995004400050002x

Vogel, T., M. Cislerova, and J.W. Hopmans. 1991. Porous media with linearly variable hydraulic properties. Water Resour. Res. 27:2735–2741. doi:10.1029/91WR01676

Vogel, T., M.Th. van Genuchten, and M. Cislerova. 2000. Effect of the shape of the soil hydraulic functions near saturation on variably-saturated flow predictions. Adv. Water Resour. 24:133–144. doi:10.1016/S0309-1708(00)00037-3

Winogradoff, D.A. 2002. Bioretention manual. Progr. Plan. Div., Dep. Environ. Resour., Prince George's County, Upper Marlboro, MD.